https://ntrs.nasa.gov/search.jsp?R=19710024679 2020-03-11T22:06:28+00:00Z

N71-34155

FINAL REPORT
Grant NGL 34-002-047
June 20, 1971

"STUDY OF RECTANGULAR-GUIDE-LIKE STRUCTURES FOR MILLIMETER WAVE TRANSMISSION"

to
The National Aeronautics and Space Administration, Washington, D. C.

CASE FILE COPY

DEPARTMENT OF ELECTRICAL ENGINEERING
NORTH CAROLINA STATE UNIVERSITY
RALEIGH, NORTH CAROLINA

FINAL REPORT
Grant NGL 34-002-047
June 20, 1971

"STUDY OF RECTANGULAR-GUIDE-LIKE STRUCTURES FOR MILLIMETER WAVE TRANSMISSION"

to
The National Aeronautics and Space Administration, Washington, D. C.

North Carolina State University
Raleigh, North Carolina

Submitted: F J Tischer

Dr. Frederick J. Tischer, Professor
Principal Investigator

PERSONNEL

Dr. Frederick J. Tischer, Principal Investigator

Mr. Lyles Adair, Graduate Student

Mr. K. K. Agarwal, Graduate Student

Mr. F. Jalali, Graduate Student

Mr. R. A. Kraft, Graduate Student

Mr. J. R. Potukuchi, Graduate Student

TABLE OF CONTENTS

INTRODUCTION

This is the final report on Grant NGL-34-002-047. It presents a brief review of the activities, of the research carried out under the grant, and of the results. It also contains a report on results of research carried out during the period October 15, 1970 to May 15, 1971 not covered by two recent progress reports dated April 2, 1971.

The objective of the research under the grant was the study of rectangular-guide-like structures for millimeter-wave transmission. Due to the similarity of the field configuration of these structures to that of the rectangular waveguide, component design based on these structures is simpler than in the case of the circular waveguide. The circular guide offers an alternative solution of the transmission problem. However, component design based on this guide is rather complex.

The structures investigated under the grant were:

1. Oversized rectangular waveguides.
2. Basic H-guide configurations.
3. H-guide with artificial dielectric.
4. The laminated-slab H-guide.
5. Microstrip line (at 35 GHz).
6. Fence guide.
7. Reflector-type waveguide.

The results of the research usually were presented in three progress reports per year.

The results of the investigation of the above waveguide configurations permit a few summarizing statements indicating the characteristics of waveguides. Oversized rectangular waveguides have comparatively low attenuation, but the existence of undesired wave modes leads to additional losses which then depend on the particular configuration of the waveguide terminals. Component design becomes difficult due to the multimode properties. The H-guide in single-mode configuration eliminates these difficulties. The dielectric losses and the losses in artificial dielectrics in the form of metal strips, studied under item 3, make this structure not yet competitive with the circular guide. Availability of a low-loss laminated dielectric, however, may change this situation. The laminated slab H-guide has an attenuation which is a fraction of that of the rectangular waveguide. The microstrip configuration with low-loss ceramics as substrates has shown prohibitively high losses (Q-values of about 200 at 35 GHz). Interesting results were obtained studying a reflector waveguide, an open waveguide composed of circular cylindrical reflectors as sidewalls (item 7). Very high Q-values were obtained under specific operational conditions (Q = 24,000 at 35 GHz). This indicates the possibility of the use as a low-loss waveguide. One of the investigated structures, the fence guide, showed promising characteristics for the design of millimeter-wave circuitry. This guide is an H-guide with the sidewalls composed of wire grids (item 6). Complete millimeter-wave circuitry can be placed on a single dielectric slab in a similar way as in the case of microstrip circuitry at

lower frequencies. Since the Q-value of the fence guide is by a factor 7 to 10 larger than that of the microstrip line, the fence guide is well applicable at 35 GHz and above. The characteristics of this guide and its use in components such as matched terminations, attenuators, and H-plane bends were investigated in greater detail under the grant. Use of the laminated H-guide for connecting antennas with transmitters and receivers and for medium distance transmission and use of the fence guide in millimeter-wave circuitry is recommended.

The research also resulted in very advanced measurement equipment used for the verification of the theoretical results. Measurement setups for high-accuracy determination of Q-values ($\pm$0.3%) and automated field plotting equipment were developed.

Present termination of the grant interrupted a system study of a millimeter-wave receiver based on the fence guide and the solution of the problem of the effects of surface roughness at millimeter waves.

The research was carried out by the principal investigator assisted primarily by students. The names of the students were listed in the progress reports. The major publishing effort consisted of progress reports containing about 1200 pages and were usually published in three issues per year. Two Masters' theses and one dissertation for a Doctor's degree were completed under the grant. They were also submitted to the sponsor as progress reports. Seminars, participations and presentations of the results in conferences, and publications in journals were parts of the activities under the grant.

FENCE GUIDE FOR MILLIMETER WAVES

By F. J. Tischer

Abstract- The fence guide is a modified H-guide particularly well suited for millimeter-wave circuitry. Essentials of the field distribution in the guide, of the characteristics, and applications of the guide are described. The concept permits design of integrated circuitry on a single dielectric slab.

INTRODUCTION

In this paper a new waveguide for millimeter waves called "Fence Guide" will be discussed. The new guide is a modified H-guide with the specific property that it can be mounted on a dielectric slab. The slab may then be the carrier of more elaborate circuitry.

The H-guide is an open waveguide which has a cross section in the form of an H [1-3]. It is composed of two parallel conducting strips running along the axis of the guide. They are separated by a central dielectric slab. In the cross section, the metallic strips form the vertical legs of the H and the dielectric slab the horizontal bar. The wave propagation in this guide is confined in the horizontal transverse direction by the reflecting metallic strips. Confinement in vertical direction is due to surface-wave propagation with the fields decreasing exponentially from the dielectric slab toward the upper and lower openings. Only a small fraction of the fields travels along the openings and radiation can be kept negligible. In the low-loss mode, the electric field strength vector in the center of the guide is parallel to the sidewalls and points in vertical direction.

The fence guide is a modified H-guide in which the solid metallic sidewalls have been replaced by metallic posts which cross a dielectric slab. The metallic posts form two parallel wire grids which run along the axis of the waveguide and serve as reflectors. Since the E-vector of the waveguide fields is parallel

to the posts, the wire grids act as effective reflectors and waveguide walls. The wire grids then keep the waves confined to the region in between. The confinement of the fields in vertical direction is due to surface wave propagation with the fields decreasing exponentially in direction from the electric slab.

The fields in the H-guide are superpositions of TE and TM wave modes since they have to satisfy the additional boundary conditions at the surfaces of the dielectric slab. The fields are those of waves propagating in hybrid modes with the magnetic field vector parallel to the boundary surfaces of the dielectric slab. In the field consideration one has to distinguish between sets of field equations for the region inside the dielectric and for the air space above and below the dielectric. As an approximation it is assumed that the parallel, reflecting walls extend to infinity. The equations for the field distributions of an H-guide have the following form:

Dielectric:

$$
\begin{aligned}
E_x &= E_0 \cos k_x x \sin k_y y \left(e^{-jk_z z} e^{j\omega t}\right) \\
E_y &= -E_0 \frac{k_x k_y}{k_e^2} \sin k_x x \cos k_y y \\
E_z &= j E_0 \frac{k_x k_z}{k_e^2} \sin k_x x \sin k_y y \\
H_x &= 0 \quad ; \qquad k_e^2 = k_y^2 + k_z^2 \\
H_y &= E_0 \frac{\omega \varepsilon k_z}{k_e^2} \cos k_x x \sin k_y y \\
H_z &= -j E_0 \frac{\omega \varepsilon k_z}{k_e^2} \cos k_x x \cos k_y y
\end{aligned}
\qquad (1)
$$

Air:

$$E_x = E_0' e^{-\alpha_x (x-d)} \sin k_y y \, (e^{-jk_z z} e^{j\omega t})$$

$$E_y = -E_0' \frac{\alpha_x k_y}{k_e^2} e^{-\alpha_x (x-d)} \cos k_y y$$

$$E_z = jE_0' \frac{\alpha_x k_z}{k_e^2} e^{-\alpha_x (x-d)} \sin k_y y$$

$$H_x = 0 \; ; \qquad E_0' = E_0 \varepsilon_r \cos k_x d$$

$$H_y = E_0' \frac{\omega \varepsilon_0 k_z}{k_e^2} e^{-\alpha_x (x-d)} \sin k_y y$$

$$H_z = -jE_0' \frac{\omega \varepsilon_0 k_y}{k_e^2} e^{-\alpha_x (x-d)} \cos k_y y \qquad (2)$$

All field components contain a term $\exp(-jk_z z)$ which stands for the wave propagation along the guide and has been omitted. We have the sinusoidal variations in the y and x directions within the dielectric. E_z and E_x are zero on the walls and have a maximum in the center. In the dielectric, E_x decreases according to $\cos k_x x$ toward the upper and lower boundary surfaces of the dielectric slab with a discontinuity at these surfaces ($D_{x1} = D_{x2}$).

In the air region, the longitudinal and transverse-horizontal field distributions are equal to those in the dielectric. In the vertical direction, the fields now decrease exponentially from the boundary surfaces toward the upper and lower openings with a constant α_x as the decay factor.

The propagation constants or wave numbers in the directions of the coordinates are related by the following characteristic equations which have to be satisfied.

Dielectric region: $k_0^2 \varepsilon_r = k_x^2 + k_y^2 + k_z^2$ (3)

Air region: $k_0^2 = -\alpha_x^2 + k_y^2 + k_z^2$ (4)

$$\varepsilon_r \alpha_x = k_x \tan k_x d \quad (5)$$

$$k_0 = 2\pi/\lambda_0 \quad (6)$$

The equations allow determination of the longitudinal propagation constant k_z. From it, the guide wavelength λ_g can be computed. Another important quantity is the decay constant α_x which describes the rate of decrease in vertical direction. The constant k_y is dictated by the spacing of the sidewalls according to $k_y = \pi/b'$.

CHARACTERISTICS OF THE FENCE GUIDE

Let us next consider two cases of sidewalls, namely, solid walls and two rows of thin conducting posts a distance b apart. Assuming good conductors, the solid walls have a surface impedance which is practically zero. If one computes the transverse surface impedance in an H-guide with solid walls, one finds that, at a small distance Δb from the wall, it has a low imaginary value. If we now place surfaces with such surface impedances at these positions on both sides of the center, we may take the solid walls away with the fields between the relative surfaces remaining the same as before. Since the surface impedances of wire grids are as an approximation, imaginary and have for closed spacing between the grids a small value, the rows of posts of a fence guide satisfy these conditions. It follows that a fence guide with the width b has field distributions and characteristics

similar to those of an H-guide with solid walls a distance b' apart. The distance b' is somewhat larger than b ($b' = b + 2\Delta b$). Figure 2 shows the geometry of the analogous structures.

The two waveguides have equal characteristics if the theoretical surface impedance at a distance $(b' - b)/2$ from the solid wall equals the surface impedance of the wire grid at the same position. Based on this concept the distance between the equivalent solid walls b' can be computed. One obtains

$$b' = b - j \frac{\lambda_0}{\pi} \frac{Z_s}{Z_0} \tag{7}$$

where Z_s is the surface impedance of the wire grid. This impedance is a function of the wavelength λ_0, diameter of the wires D', and spacing between wires s,

$$Z_s = j F(\lambda_0, D', s) \quad ; \quad Z_0 = \sqrt{\mu_0/\varepsilon_0} \tag{8}$$

This, in turn, permits determination of the guide wavelength, which becomes, as an approximation in normalized form

$$\frac{\lambda_g}{\lambda_0} = \frac{\lambda_g^{(H)}}{\lambda_0} + j \frac{Z_s}{4\pi Z_0} \left(\frac{\lambda_g^{(H)}}{b} \right)^2 \tag{9}$$

In this equation $\lambda_g^{(H)}$ is the guide wavelength for the H-guide if the wire grids are replaced by solid walls a distance b' apart. We observe that the guide wavelength is somewhat smaller for wire grids since Z_s is positive and imaginary.

The attenuation of the fence guide consists of contributions by the dielectric losses in the slab, conduction losses in the wire grids, leakage through the grids and radiation through the

openings on top and bottom. Optimum operational conditions can be obtained by choosing proper values of the thickness of the dielectric slab, of the diameter of the conducting posts, and their separation. The height of the posts has to be properly chosen also. Measurements of the Q-value of shorted sections of the fence guide at 35 GHz gave values of up to 2000. Comparison with the value of a few hundred for strip lines indicates that the attenuation is a fraction of that of microstrip lines in the same frequency range.

APPLICATIONS

Components such as power dividers, directional couplers, hybrid rings, resonators, and other circuit elements can be designed with the fence guide as a basis. As a consequence complete fence-guide circuits can be placed on a single dielectric slab in a similar manner as it is done with microstrip circuits at lower frequencies. Since the cross-sectional dimensions of the guide are in the order of magnitude of standard waveguides, tolerance problems at the design of circuits are not as severe as in the case of microstrip circuitry. The small dimensions of the guide and of components at millimeter waves and the structural form make circuitry very practical and suitable for mass production.

REFERENCES

[1] F. J. Tischer, "A Waveguide Structure with Low Losses", Arch. Elektr. Ubertragung, Vol. 7, 1953, pp. 592-596.

[2] _____ , "The H-Guide a Waveguide for Microwaves", 1956 IRE Convention Records, pt. 5, pp. 44-47.

[3] M. Cohn, "Propagation in a Dielectric-Loaded Plane Waveguide", IRE Transactions, Vol. MTT-7, 1959, pp. 202-207.

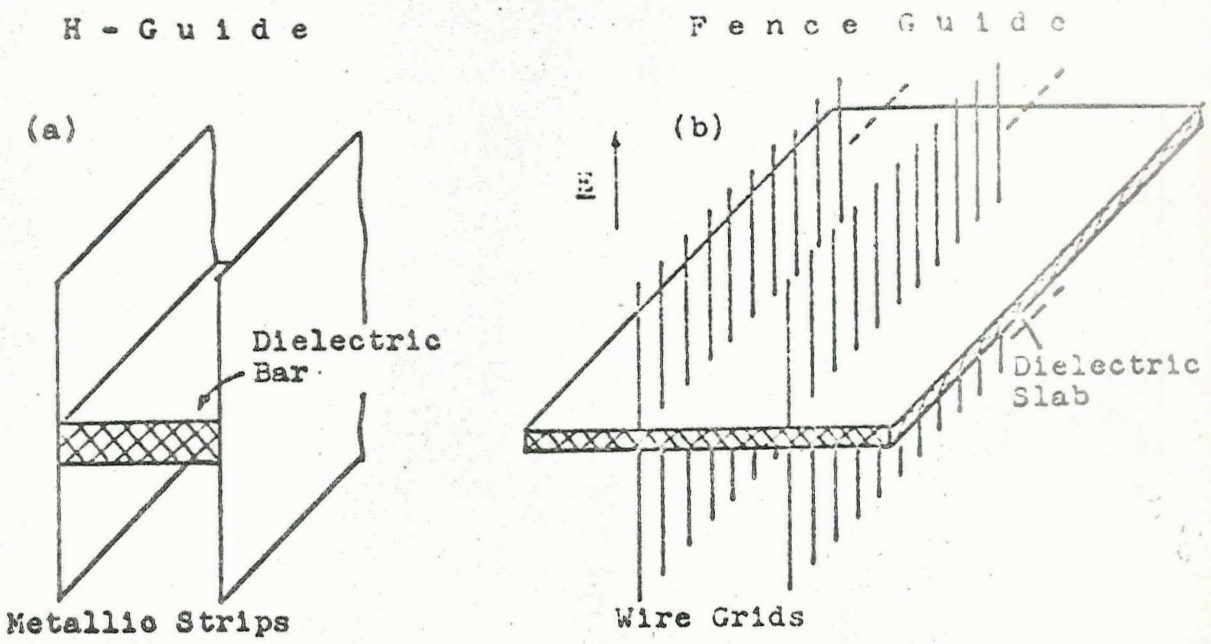

Fig. 1. Waveguide structures. (a) H-guide. (b) Fence guide.

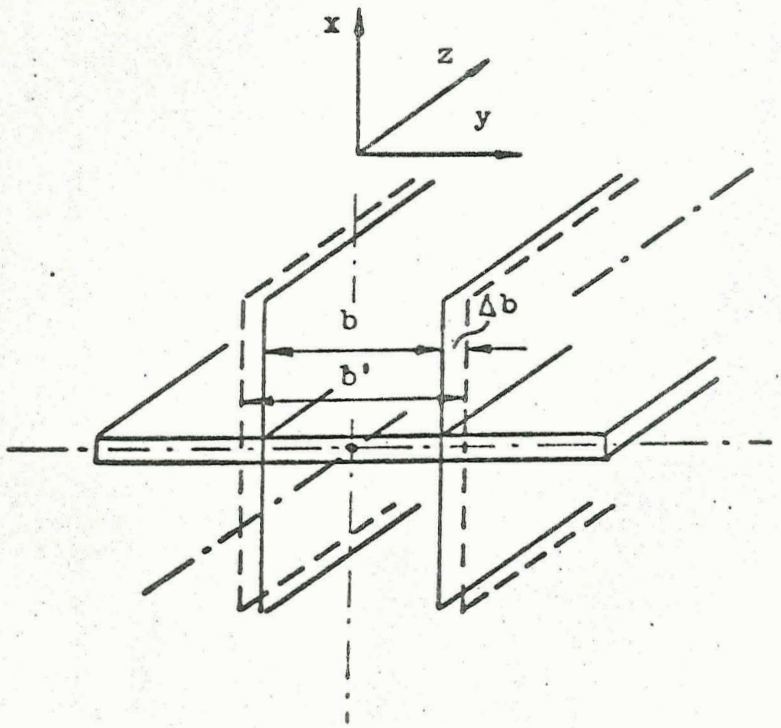

Fig. 2. Equivalent widths of waveguides.

MEASUREMENTS ON MATCHED FENCE-GUIDE TERMINATIONS

Abstract

A study of terminating a fence-guide in a reflectionless way was made. Measurements were conducted using Eccosorb foam dielectric materials in matched fence guide terminations with varying material thickness and lengths. Terminations with linear, exponential, inverted exponential tapers were fabricated from Eccosorb foam and their performance was compared at 34-36 GHz. Voltage-standing-wave ratios of less than 1.1 were obtained with linearly tapered terminations. Measurements were made on linearly tapered terminations of different lengths. Included in the appendix are measured values of the complex dielectric constants of Rexolite, Balsa wood, and Eccosorb foam.

MEASUREMENTS ON MATCHED FENCE-GUIDE TERMINATIONS

The concept of impedance matching for maximum power transfer in circuits is well known. In waveguides and coaxial lines matched conditions are needed to eliminate the mismatch errors in measurements. Wide-band terminations are therefore needed which absorb completely the incident wave without reflection or as little reflection as possible. Under these conditions the voltage standing wave ratio is low. These terminations could be fixed or adjustable and are very useful at the evaluation of line discontinuities and components. Termination elements for conventional waveguides are commercially available which result in low VSWR's down to 1.01 over a wide frequency band. These terminations, when used in the fence guide[1], gave rather poor performance and VSWR's of 4-5 dB were measured at 35 GHz. Efforts were then made to design a simple termination for low VSWR suitable in fence guide applications.

There is little theoretical treatment of matched terminations[2,3]. The design is usually based on fashioning the dissipative materials by cut and trial. The design procedure, therefore, requires a material that can be easily cut and machined. The condition of low VSWR requires that most of the incident power is absorbed in the termination and only a small fraction reflected. The material, therefore, should have a high enough loss tangent. The shape of the termination should be such that it causes a gradual change in the waveguide impedance, causing no reflection. The shape and length of the termination may be

experimentally determined.

Some measurements were made to determine complex dielectric constants of materials at 35 GHz (Appendix A). Of the materials measured, Eccosorb form (Emerson and Cuming, Inc., Canton, Mass.) ($\varepsilon_r' = 1.587$, $\varepsilon_r'' = 0.0896$) was found to be the most suitable material for use in terminations.

Measurement Setup

The block diagram of the measurement setup used is shown in Fig. 1. A 35 GHz A-band klystron is used with a power supply (Narda 62A1). The klystron output is fed through an isolator, variable precision attenuator and frequency meter to a TRG-slotted line and the field strength measurement setup. A fence guide ($s_w = 1.016$", 6.75" long) is placed in the setup and connected to the end of the slotted line. The probe output is fed to a detector unit and the rectified signal is fed to a VSWR meter. The dielectric material is placed in the fence guide. The output end 'A' of the fence guide is connected to a detector. The input VSWR and the output power are measured using a standing wave meter (GR-1234).

Measurement of Attenuation

Attenuation measurements were made on rectangular strips of Eccosorb foam at 35 GHz to study the effect of change of thickness. The fence guide was loaded with two strips (symmetric loading) and only one strip (asymmetric loading). The measured input VSWR is as shown in Fig. 2. As can be observed from the plots the basic behavior does not change with one or two strips

of loading and in both cases there is a region of thickness where input VSWR is less than 1 dB. The transmitted power was more than 50 dB below the input power. Measurements were then made on a sample of thickness 0.14", which falls in this region of low VSWR. Input VSWR and attenuation were measured for varying lengths of the absorbing material using two strips for loading. This is shown in Fig. 3(a,b). The input VSWR was measured between 1 and 2 dB. The insertion loss variation was around 14-15 dB for lengths up to 1.1", however, it showed a steady increase for greater length.

Measurements of input standing waves for different frequencies were made for two strip and four strip (step) loading. The thickness of each strip was 0.1". A plot for the region from 34-36 GHz is shown for the two cases in Fig. 4. The input VSWR for the step configuration was slightly lower at both, the lower and upper frequency ends; however, double strip loading had lower VSWR around the center band. In both cases, the VSWR increased to around 2.0 dB at the upper frequency end.

Measurements on Terminations

To obtain a good termination, its shape should be such that it provides gradual impedance transformation. The following three shapes (Fig. 5) were considered suitable:

(1) Linear taper

(2) Exponential taper

(3) Inverted exponential taper

The corresponding terminations were made of Eccosorb foam. The height of the termination element was up to the edge of the

fences (h = 0.58") and the width was chosen to completely fill the width of the guide. The total length of each termination was 1.6". With the termination in place, the power transmitted at the output of fence guide was more than 50 dB below the input level for the three terminations. The output of the fence guide with termination in place was shorted with a copper plate and the input standing wave ratio was measured from 34.0 - 36.0 GHz (Fig.6) for the three terminations. A VSWR of 0.4 dB (power ratio 1.096) was measured for the linear taper. Some typical figures are given in Table I below for the three terminations.

Table I

VSWR Values of Terminations

	Termination width		
	Linear Taper	Exponential Taper	Inverted Exponential Taper
VSWR(dB) at 34.0 GHz	1.60	2.0	1.78
VSWR(dB) at 35.0 GHz	0.36	0.77	0.60
VSWR(dB) at 36.0 GHz	1.80	2.20	1.72
Bandwidth(GHz) for VSWR 0.8 dB or less	1.04	0.95	0.42

Of the three terminations tested, the linearly tapered termination had low standing waves over the widest frequency band.

Further measurements of input VSWR at 35.0 GHz were made on linearly tapered terminations of varying lengths L, placed as shown in Fig. 5(a) (configuration 1) and as shown in Fig. 5(d)

in inverted form. A diagram of the measured data for the two configurations are shown in Fig. 7. Two observations can be made from the plot.

(1) For small length of the taper, the standing wave ratio is high for both cases. With increased length of the taper, the VSWR goes down until for large taper lengths, the VSWR again shows an increase.

(2) The VSWR for the tapered form is generally higher than for the inverted linear tapered element over the low VSWR region of length. This was further confirmed by using terminations of Balsa wood with embedded carbon. The input VSWR of a linearly tapered termination was measured to be 9.5 dB which was reduced to 5.4 dB for inverted linear taper due to exponential decay. The field at the edge of the fence is about 15 dB below the field at the dielectric level. In the inverted taper form, the absorbing material is in the lower-field region at the input and hence the impedance transformation is much more gradual than in the other configuration.

The above studies have demonstrated that terminations with low standing waves and reasonable bandwidth can be designed for fence guides at 35.0 GHz. The study continues on terminations using rigid absorbing material.

APPENDIX

Measurements on Dielectrics

The complex dielectric constant of materials at microwave frequencies can be obtained with reasonable accuracy by placing the dielectric sample in a short circuited waveguide at the shorted end and by measuring the guide wavelength and the standing wave ratio with and without the dielectric sample. Considerable simplification is obtained by choosing the length of the dielectric sample such that a minimum lies in the input face of the sample. The losses of the dielectric have then essentially no effect on the guide wavelength of the dielectric-filled guide. The following expressions can be derived using transmission line techniques[4].

$$\varepsilon_r' = \left(\frac{\lambda_o}{\lambda_c}\right)^2 + \left(\frac{\lambda_o}{\lambda_{g\varepsilon}}\right)^2 \tag{1}$$

$$\varepsilon_r'' \simeq \frac{1}{VSWR}\,\frac{2}{\pi}\left(\frac{\lambda_o}{\lambda_{g\varepsilon}}\right)^2 \frac{\lambda_g}{\lambda_{g\varepsilon}} \tag{2}$$

where $\varepsilon_r = \varepsilon_r' - j\varepsilon_r''$, (3)

and λ_o = free space wavelength,

λ_c = cutoff wavelength of the waveguide,

λ_g = guide wavelength,

$\lambda_{g\varepsilon}$ = guide wavelength of dielectric-filled guide,

VSWR = standing wave ratio

For increased accuracy and to account for increased guide losses

$$\frac{1}{VSWR} = \frac{1}{VSWR_1} - \frac{1}{VSWR_2}$$

where $VSWR_1$ = the standing wave ratio with dielectric in the waveguide.

$VSWR_2$ = the standing wave ratio without dielectric in the waveguide.

In the measurements, a rectangular waveguide (WR-28) was used with a TRG-slotted line. Probe insertion was kept at the minimum. Using some preliminary information of ε_r', the guide wavelength $\lambda_{g\varepsilon}$ was read of the plots, Fig. 8(a) and Fig. 8(b). The sample was cut to tightly fit the inside of WR-28. To arrive at the proper length, a method of cut and trial was used. Starting with a sample length nearly as much as $\lambda_{g\varepsilon}$, the sample length was reduced and the position of two consecutive minima was measured until the change in sample length did not change the position of the minima. Then

$$\lambda_{g_\varepsilon} = 2\left\{\frac{\lambda_g}{2} - \Delta x\right\}$$

where

Δx = total shift in the minima i.e. from empty guide to the final position of minima.

Measurements were made on Rexolite, Balsa wood and Eccosorb foam at 35.0 GHz. The following results were obtained.

Table II

Material	Measured $\lambda_{g\varepsilon}$ (mm.)	ε_r'	ε_r'
Rexolite	5.830	2.5209	0.002566
Balsa wood	9.900	1.2280	0.00115
Eccosorb foam	7.740	1.5870	0.08960

The accuracy of the method is limited by the accuracy of the determination of $\lambda_{g\varepsilon}$ and the sample preparation.

References

1. Dr. F. J. Tischer, K. K. Agarwal: Comparative Study of Fence Guide Fields, Progress Report, Grant NGL 34-002-047, N. C. State University, (October 15, 1970).

2. R. C. Ellenwood, W. E. Ryan: A UHF and Microwave Matching Termination, Proc. of IRE, pp. 104-107, (January 1953).

3. G. C. Clemens: A Tapered Line Termination at Microwaves, Quarterly Applied Math. Vol. VII, No. 4, pp. 425-432 (January 1950).

4. Dr. F. J. Tischer: Microwave Measurement, Springer-Verlag, Berlin (1958).

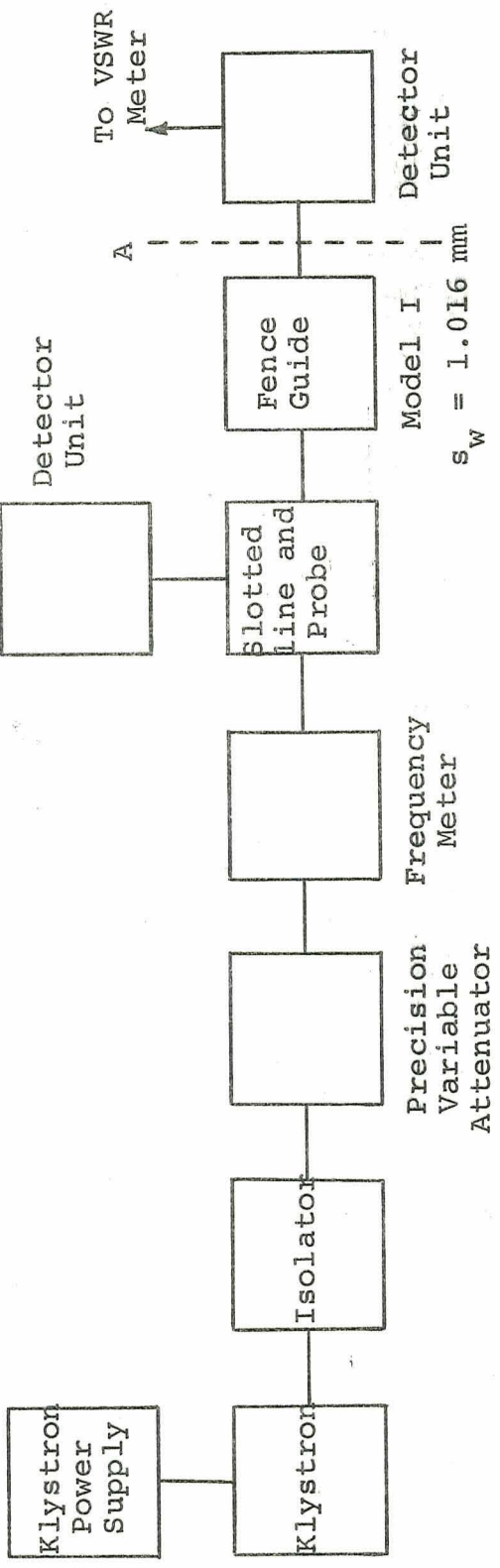

Fig. 1 Measurement Setup

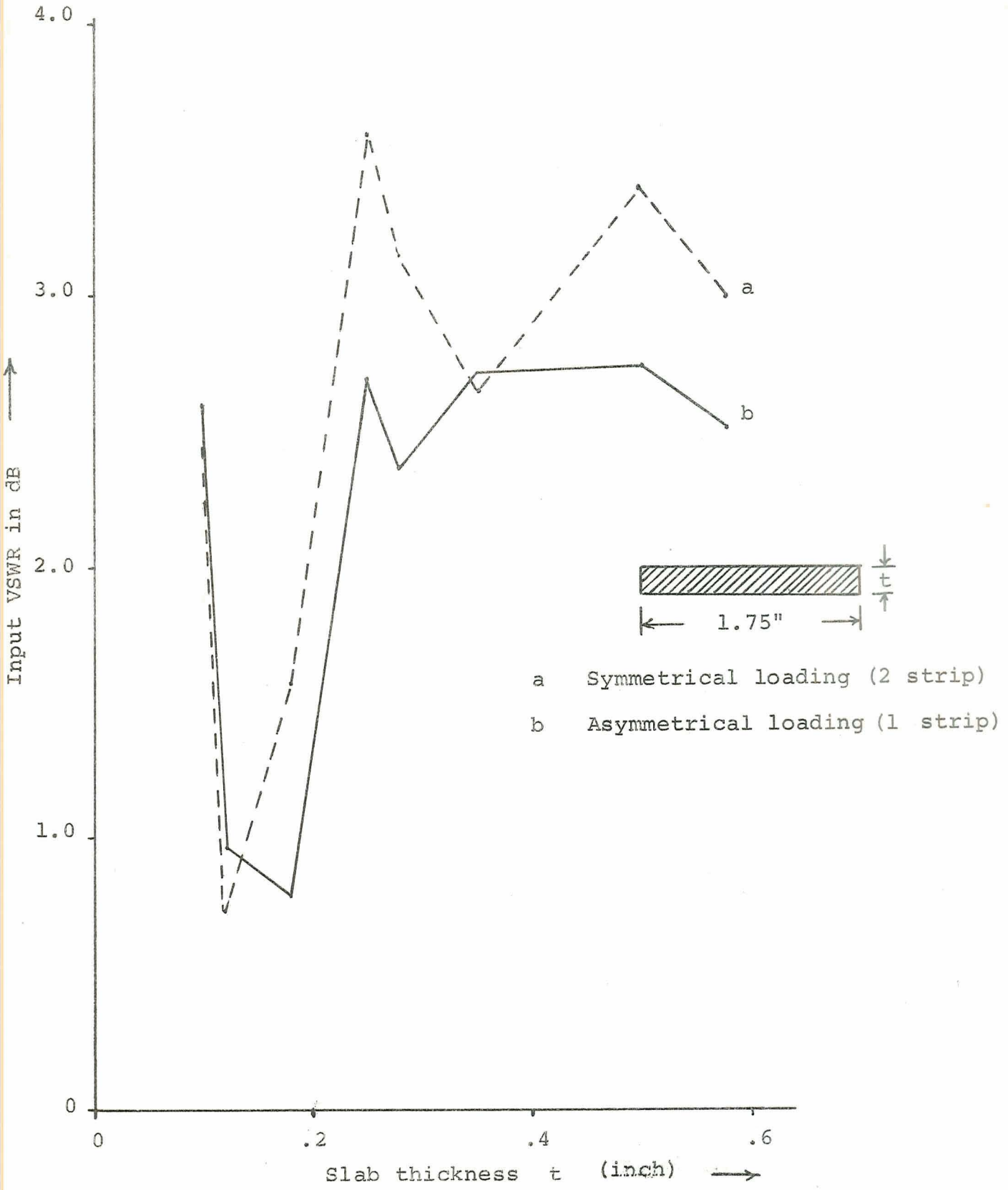

Fig. 2 Input VSWR variation with thickness of foam material in fence guide at 35 GHz.

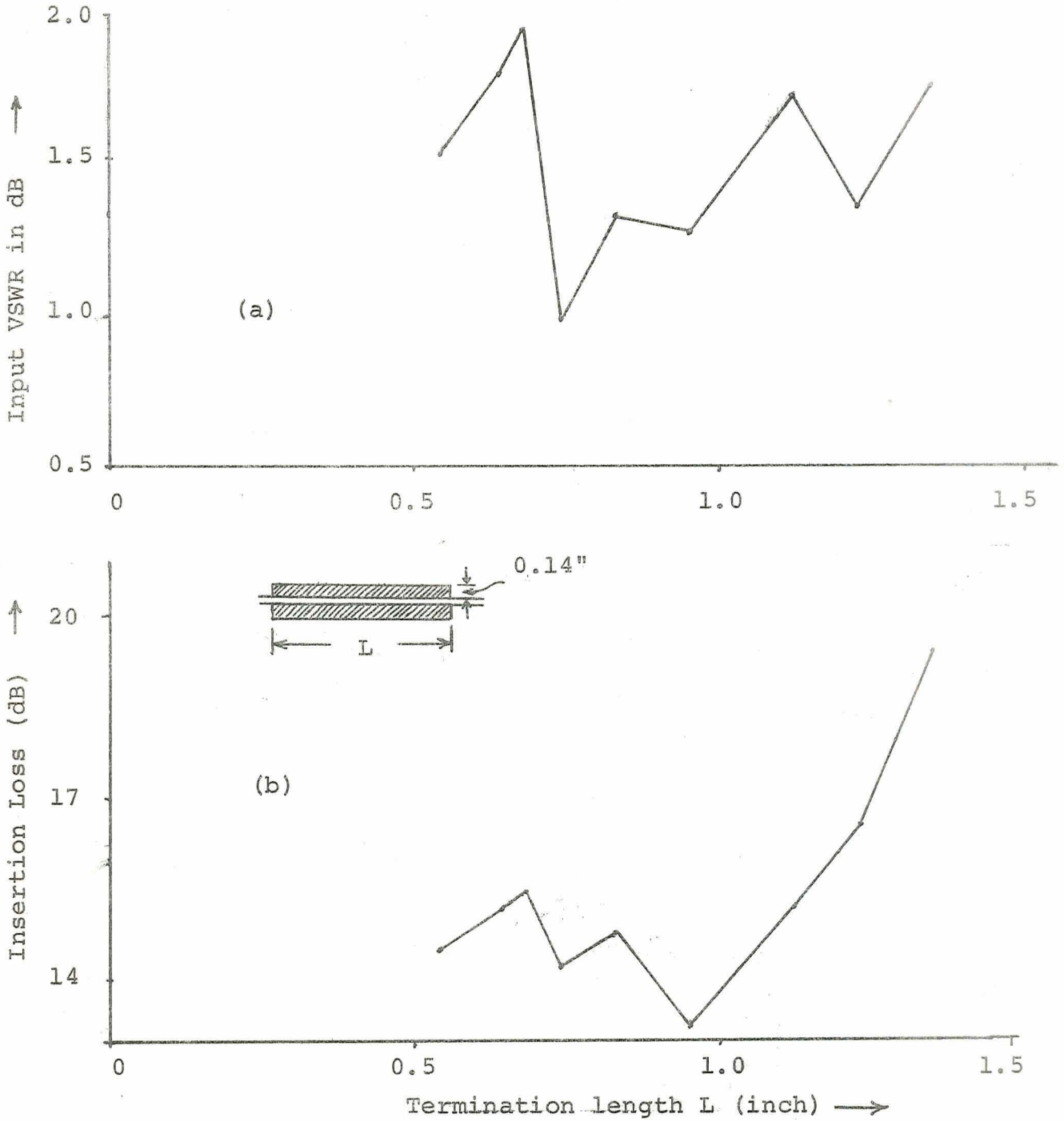

Fig. 3 Insertion loss and input VSWR variation of a single slab termination at 35 GHz for varying length of the slab.

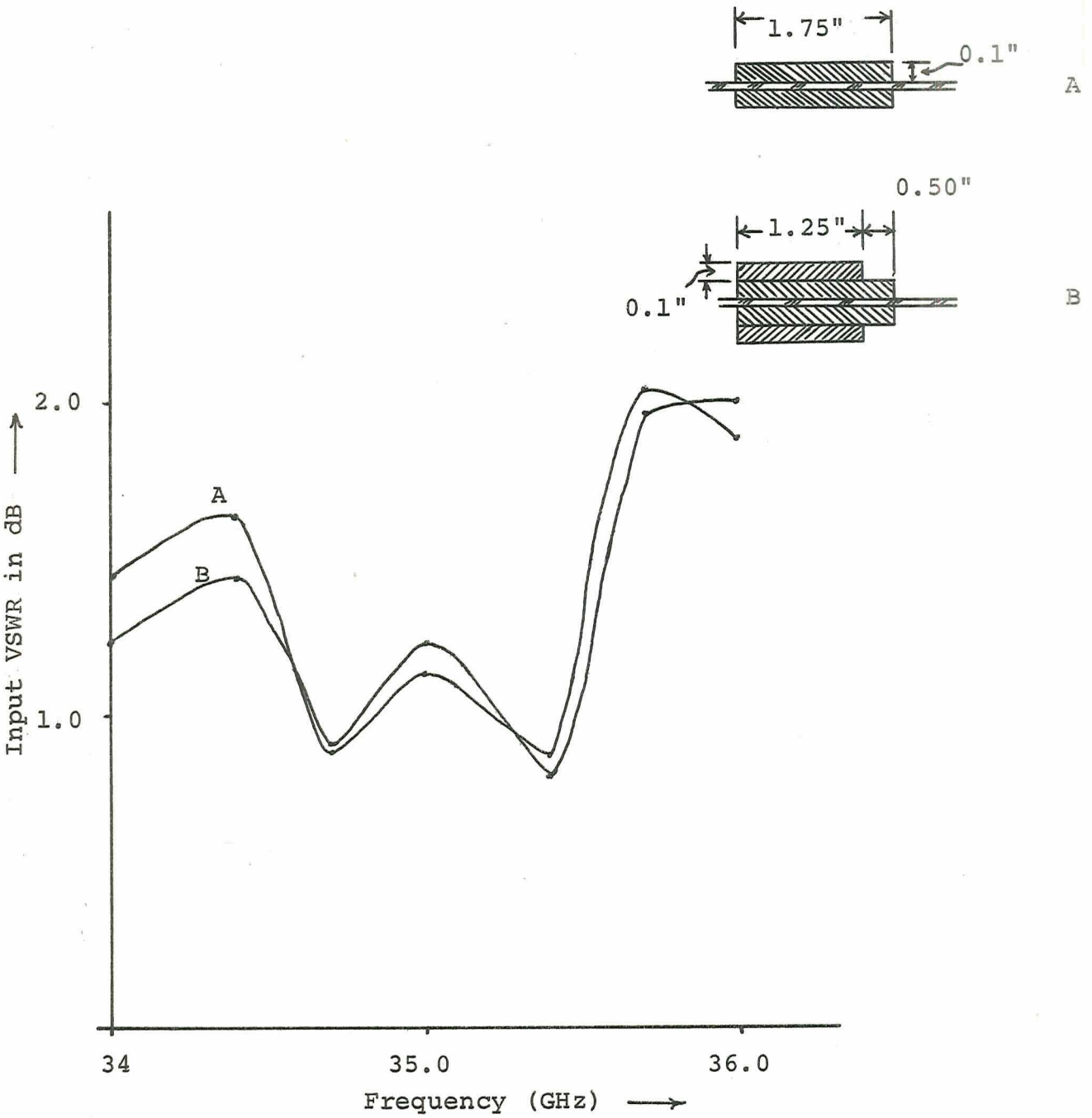

Fig. 4 Frequency dependence of the input VSWR for termination with

A. Single slab
B. Double Slab

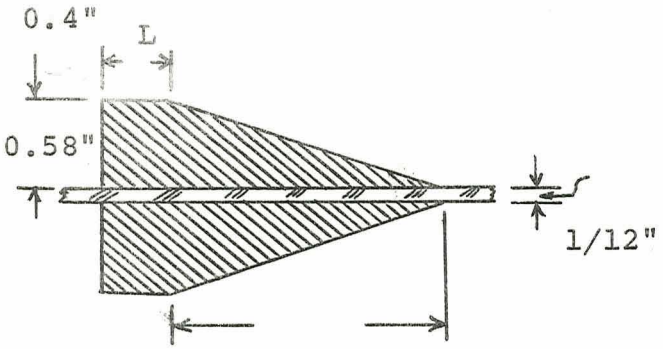

L = 1.2"

(a) Linear taper

Eccosorb
Foam

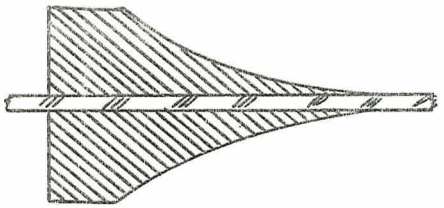

(b) Exponential taper

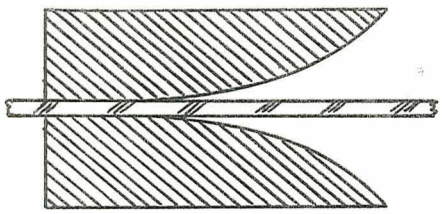

(c) Inverted exponential taper

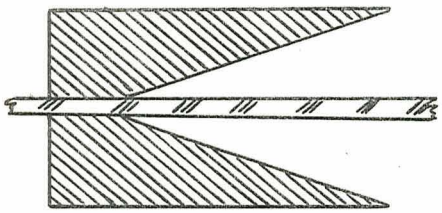

(d) Inverted linear taper (alternate arrangement)

Fig. 5 Various shapes and arrangement of terminations.

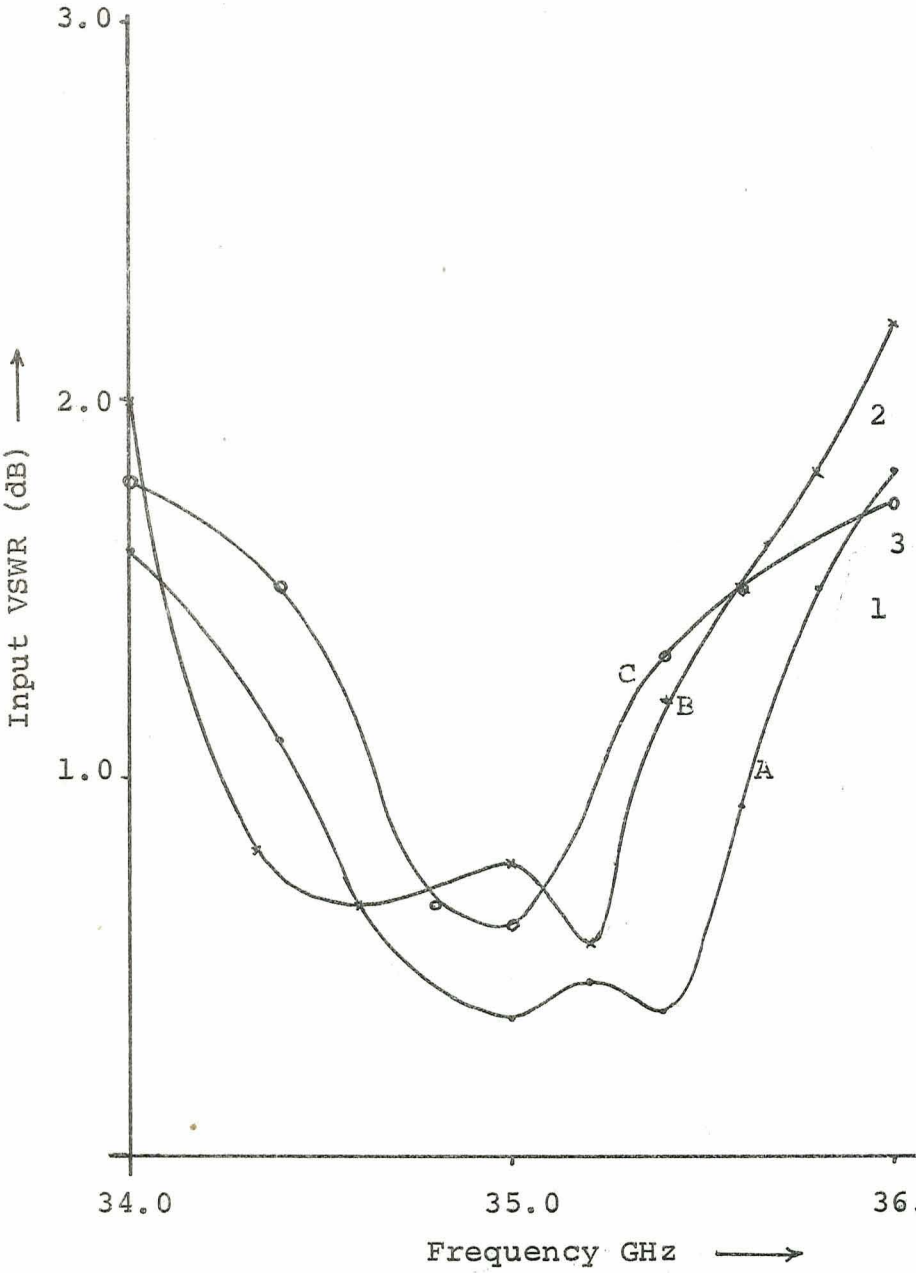

Fig. 6 Frequency dependence of the input VSWR of terminations with:
A Linear taper
B Exponential taper
C Inverted exponential taper

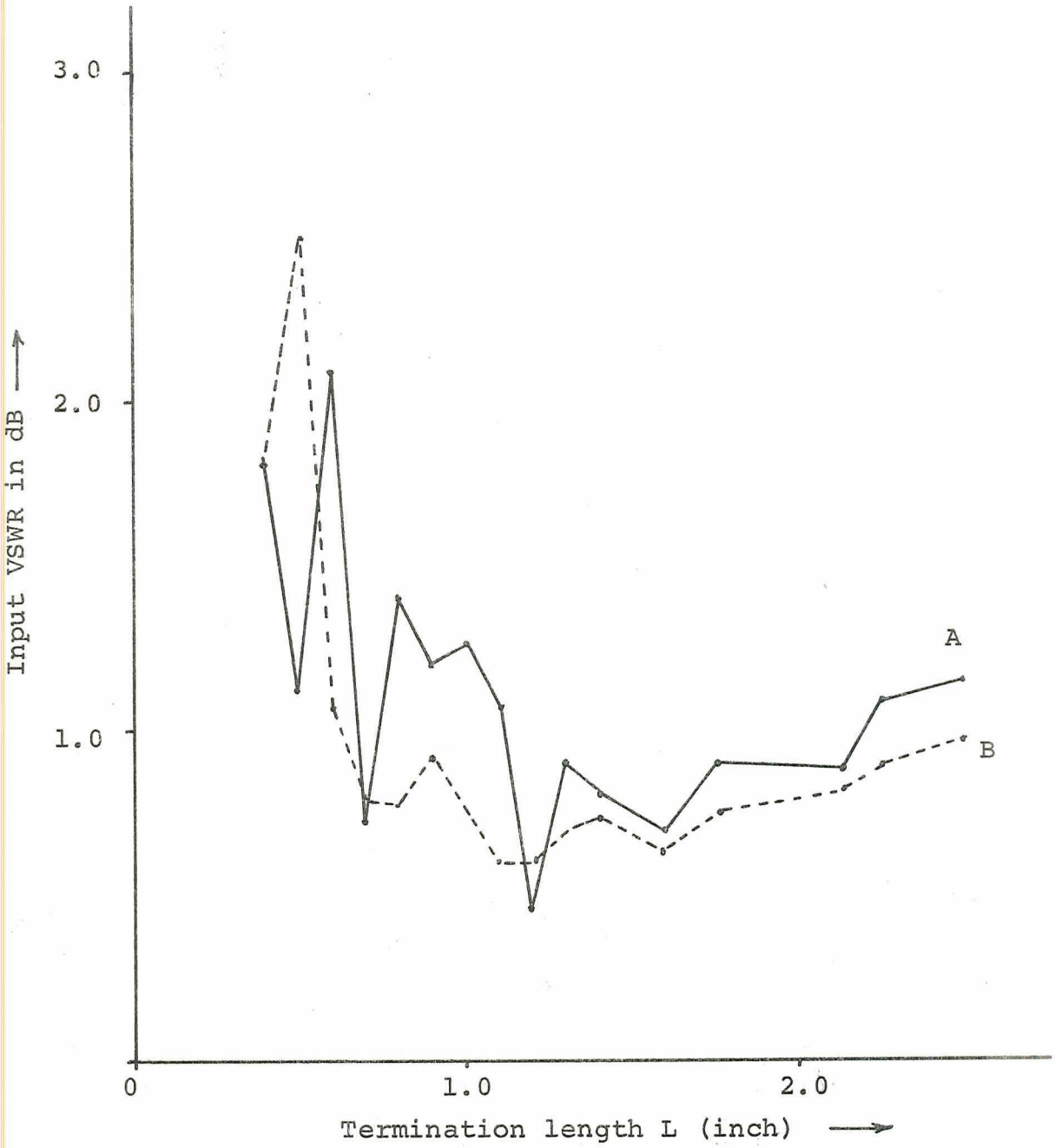

Fig. 7 Input VSWR vs. length of the tapered termination at 35.0 GHz.

A Linear taper
B Inverted linear taper

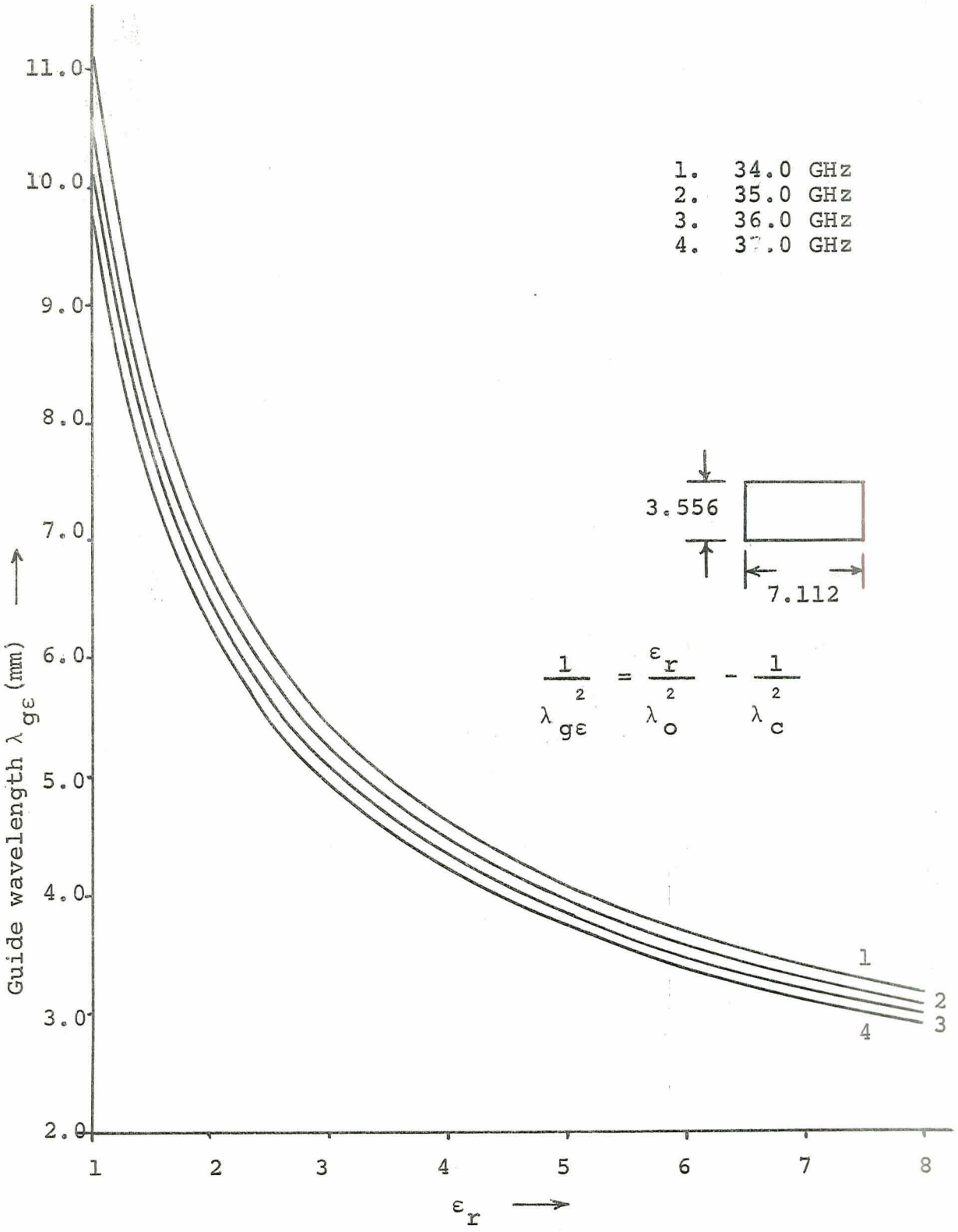

Fig. 8a Guide wavelength for a dielectric-filled rectangular waveguide.

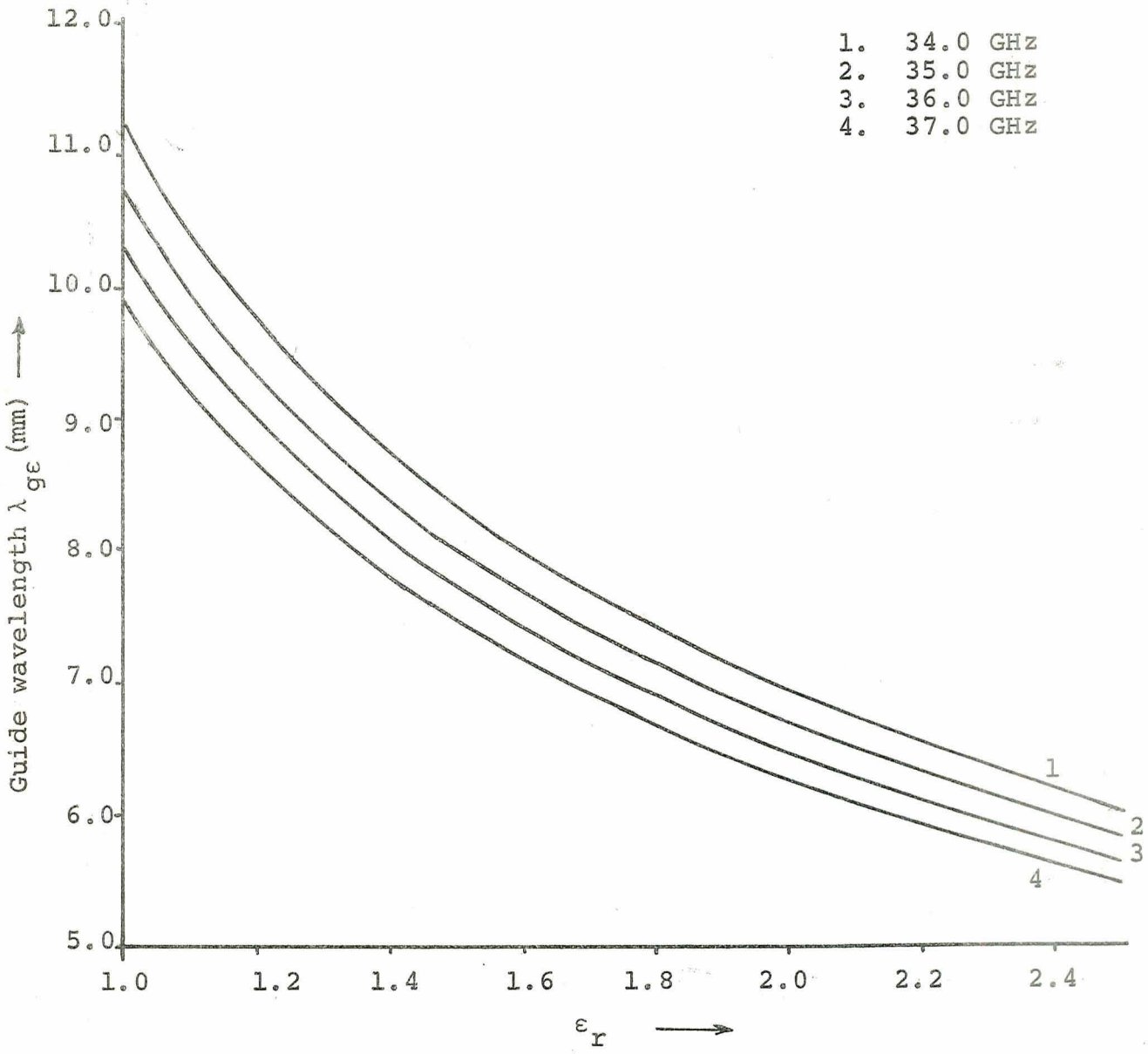

Fig. 8b Guide wavelength for a dielectric-filled rectangular waveguide.

EXPERIMENTAL STUDY OF A NON-CONFOCAL CYLINDRICAL RESONATOR

Abstract

An experimental investigation of a non-confocal resonator with cylindrical reflectors using two different types of coupling energy is reported. In one case the resonator was operated as a transmission cavity with end-wall coupling and in the second case as a reflection type cavity with energy coupled through one of the reflectors. Measurements were made of the field distribution, mode numbers, and the quality factor for varying separation of the reflector walls at three different frequencies. The dependence of the Q-value on the mode numbers is discussed. It is also shown that the theoretically computed resonance frequencies of an equivalent rectangular cavity compares well with the measured values of the curved-wall open resonator.

Introduction

The possibility of instabilities in confocal resonators using two reflectors, unless very rigid tolerances at the manufacture of the reflectors and uniformity of spacing were maintained, has been reported in the literature[1]. It was also reported that non-confocal systems generally lead to unsatisfactory operation and low Q-values. This was not confirmed in our measurements and it was reported earlier[2] that these problems can be overcome by a modified resonator geometry with two flat side walls.

It was observed that this structure for non-confocal spacing can give high Q-values up to 40,000. Resonances with Q-values of this order were realized even with spacing between the reflectors of one-eighth of their radius of curvature. This resonator has then the advantage of a high Q-value with a considerably reduced size. Details of the measurements conducted on this resonator are described in the next section.

Measurements on a Reflector-Type Resonator

Extensive experiments were conducted, over a wide range of spacing d between the reflectors, of a cavity as illustrated in Fig. 1. Three different frequencies were chosen at which the field distributions were measured in the cavity. The setup used for this purpose is shown in Fig. 2. A small compensated movable probe and an xy plotter were used for obtaining the field plots. As expected, a standing wave pattern was observed in the y and z directions in all cases. Field distributions across the resonator (x-axis) were checked at these frequencies and they were found to be Gaussian. Field plots showed that the characteristics of the Gaussian distributions vary with the spacing between the reflectors. The components of the electric field in the x direction (E_x) can be expected to be basically of the form

$$E_x = e^{-\frac{x^2}{2a^2}} \sin k_y y \sin k_z z \quad , \qquad (1)$$

where K_y and K_z are the wave numbers in the y and z directions respectively.

Considering an equivalent rectangular cavity with flat walls and using E_x as the principal field component, the other components can be calculated for a TE mode. The resonance frequency of the cavity is then given by

$$f_0 = \frac{c}{2}\sqrt{\left(\frac{n}{d}\right)^2 + \left(\frac{p}{l}\right)^2} \qquad (2)$$

where

n,p are the mode numbers in the y and z directions respectively,

d is the distance of separation of the flat walls substituted for the curved reflectors, and

l is the length of the cavity.

The resonance frequency was calculated for each mode using Eq. 2 and the mode numbers from the field plots. Although Eq. 2 is derived from considering the equivalent cavity with plane walls, it was noticed that the computed values of frequency differed only by about one per cent from the accurately measured values. If the separation of the equivalent plane walls was chosen as indicated in Fig. 3, measurement at three frequencies exhibited a similar agreement. The results obtained for three frequencies are shown in Fig. 4. At the computation of the resonant frequency the mode number along the x-axis was taken as zero as the distribution was Gaussian. Similar agreement is expected to hold even if the distribution along x-axis is of the form of a Hermite function and E_x represented as

$$E_x \quad e^{\frac{x^2}{2a^2}} H_m\left(\frac{x}{a}\right) \sin k_y y \sin k_z z$$

The term $e^{-x^2/2a^2} H_m(x/a)$ is a Hermite polynomial of order m. In this case m represents the mode number in x direction.

The technique used in measuring Q-values and the dependence of Q on the mode numbers will be discussed at the end of the next section.

Measurements on a Transmission-Type Cavity

In the present case the energy was coupled into the resonator through a small circular hole in the side wall as shown in Fig. 3. The size of the aperture for obtaining good resonance patterns and high insertion losses of the order of 40 dB was determined experimentally. High insertion loss was preferred to ensure that the unloaded Q would be approximately equal to the loaded Q-value.

For measuring the Q-values, a Klystron source operating at about 35 GHz was swept through the resonance range by means of an external modulating unit and the 3 dB points of the resonance output curve were measured with the help of frequency markers generated by mixing the A-band signal with the 4th harmonic of a stabilized X-band signal and monitoring the frequency of the X-band signal with a counter. As in the previous case the mode numbers were evaluated from the field plots.

From the knowledge of Q-values of the resonator the attenuation can be computed. It can be shown that the attenuation and the Q are related by the expression

$$A\,[dB] \quad \frac{8.68\pi d}{Q}$$

where $A^{[dB]}$ is the attenuation in dB per reflection.

Before the diffraction losses can be found from the measured data, it is necessary to account for conduction losses in the metallic reflectors. A TE mode was assumed to exist in the resonator, and considering Eq. 1 for E_x as the principal mode, the other field components were obtained. From these equations the conduction losses were computed.

The magnitudes of the attenuation were many orders less than those computed from the Q factor. This implies that the conduction losses can be disregarded and that the diffraction losses can be obtained as a first approximation directly from Eq. 3.

Figures 5,6,7 show the results of the measurements. They indicate the dependence of Q on the mode numbers. In Figure 5, which shows the dependence of Q on the mode number p, each line represents the range of the Q-value measured with the same mode number p for various distances of separation between the reflectors. Each point marked on the line also corresponds to a different mode number n with same p. Fig. 6 shows the dependence of Q on n. As in the previous case each line here represents the range of Q-values measured for constant number n as spacing is varied and each point on this line represents a mode with a different p. The following conclusions can be drawn from the plots:

(1) For a fixed p the Q-value is highest for a specific number n. In this case n = 19 for p = 11 and it drops off for increasing values of n.

(2) For fixed numbers n (see Fig. 6), smallest numbers of p correspond to highest Q. For larger numbers of p, the Q-value decreases rapidly. The highest value of the measured 'Q' was for n = 19 and p = 11. It was, however, noticed that the same pair of mode numbers was experimentally observed at more than one value of d. In such cases the mode with smallest d gave highest Q.

The latter phenomena can be observed from Fig. 7. It shows the dependence of 'Q' on 'p' and d for constant numbers n. The vertical lines of the plots appearing for lower value of p represent the ranges of the Q-value for the modes with the same numbers n and p but for different distances of separation d. In all these cases it was observed that highest 'Q' was obtained for smallest separation d.

Measurements conducted at the two other frequencies (37.508 and 37.49 GHz) indicated similar trends confirming the above conclusions. The mode number n where 'Q' was highest was, however, found to be dependent on the frequency of operation. It was found that at 37.508 GHz Q was a maximum for n = 17 and for a frequency of 37.490 GHz n was 20 for the maximum Q. In all the above three cases the separation d between the reflector walls d was varied between 6.8 and to 13.5 cm.

Considerable difficulties were encountered at the measurements using the resonator as a reflection type one-port with the coupling hole at the center of one of the reflectors. This permitted d to be varied over a much wider range, 1.5 to 13.5 cm.

In this case Q-value measurements were made by evaluation of the probe output. Since the probe insertion into the resonator had to be kept small to avoid any perturbation effects, measurements could be conducted on them as the output of the probe in such cases was too small. Also, the mode number p in all these cases was very small (of order 2) and the patterns recorded were considerably distorted, not permitting the correct evaluation of p values. In the present investigations measurements were restricted to modes with moderate to low Q-values. The results for these modes compared favorably with those obtained in the first case. The conclusions are applicable for this case also. Further investigation of the structure including measurements on modes with high Q-values is now in progress.

References

1. R. W. Zimmerer: Spherical Mirror Fabry-Perot Resonators, IEEE Trans. on Microwave Theory and Technique, Vol. MTT-II, pp. 371-379, (September 1963).

2. J. R. Potukuchi, F. J. Tischer: Study of Open Resonator with Cylindrical Reflections, Progress Report, Grant NGL 34-002-047, pp. 59-66, (June 1970).

3. J. B. Beyer, E. H. Scheibe, Loss Measurements of the Beam Waveguide, IEEE Trans. on Microwave Theory and Technique, Vol. MTT-II, pp. 18-21, (January 1963).

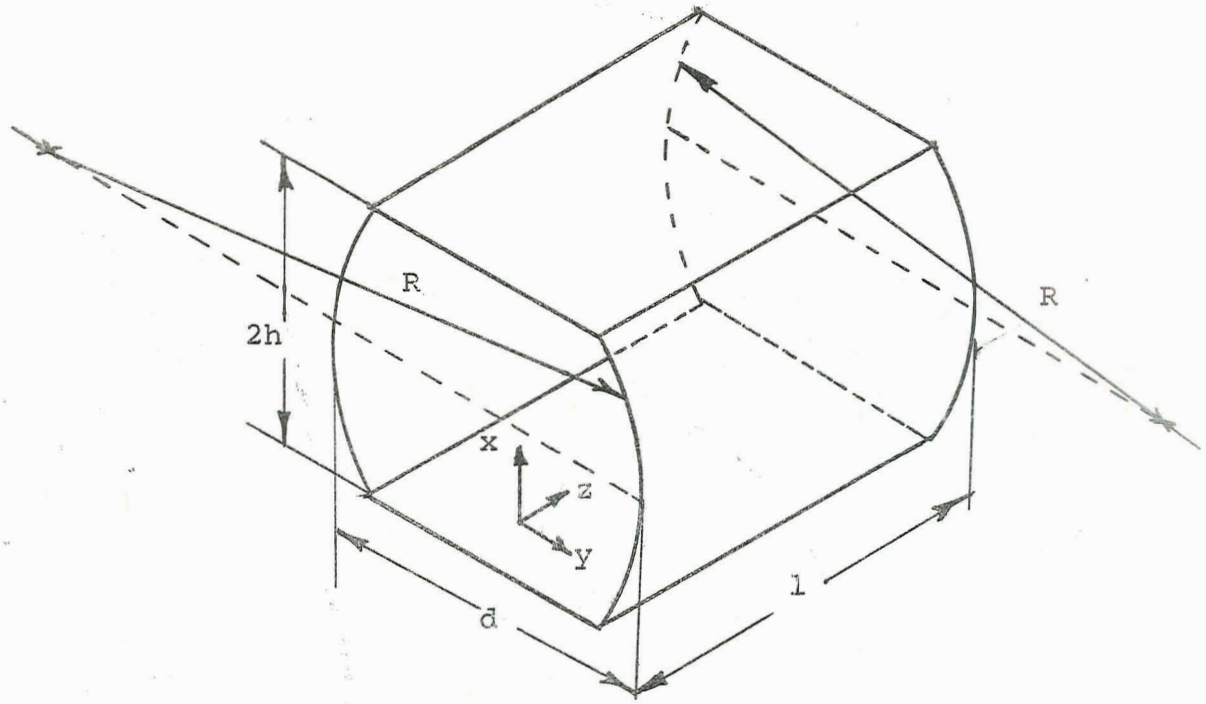

Fig. 1 Nonconfocal Resonator.

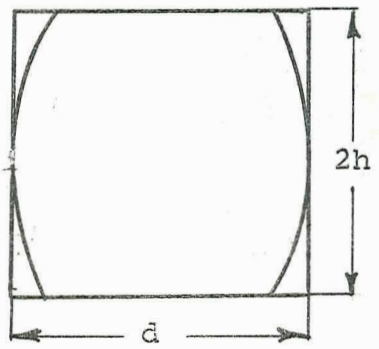

d Spacing between reflectors

R Radius of curvature of reflectors.

Fig. 3 Equivalent Plane Wall Resonator.

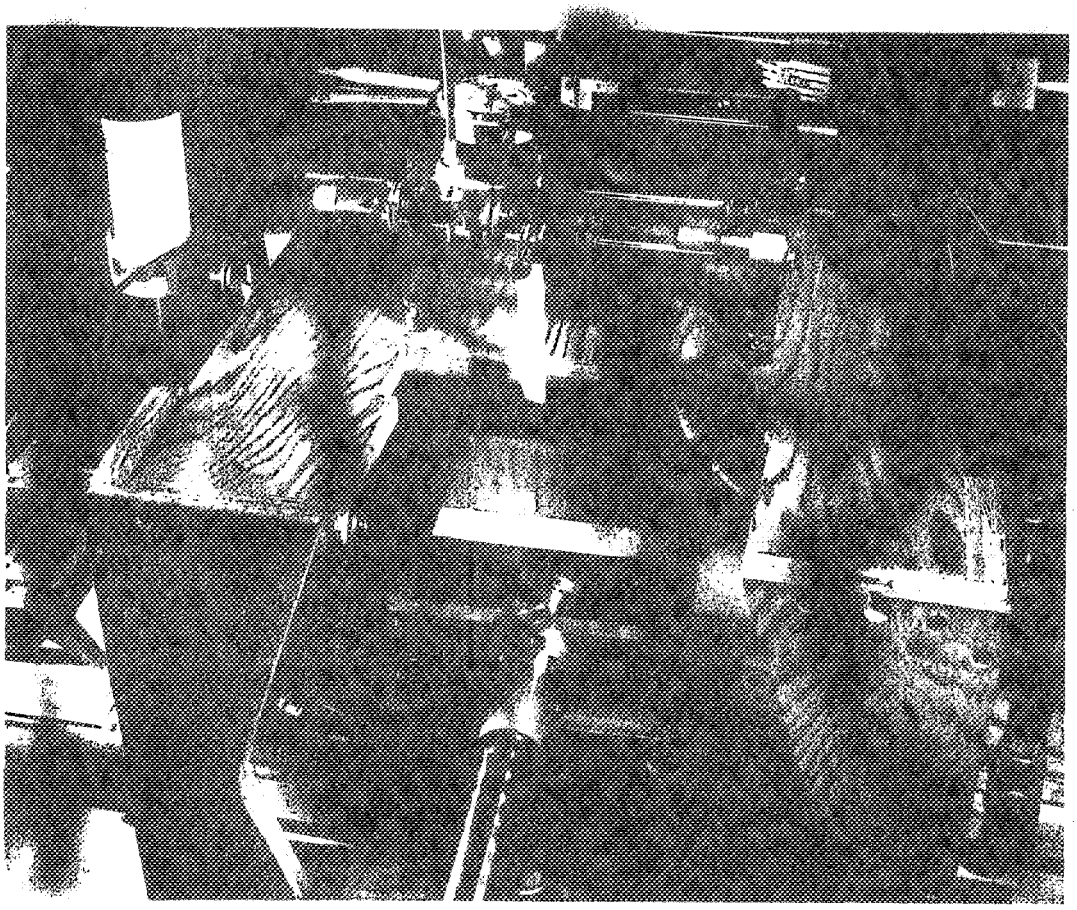

Fig. 2 Measurement setup for the study of an open cylindrical-reflector resonator.

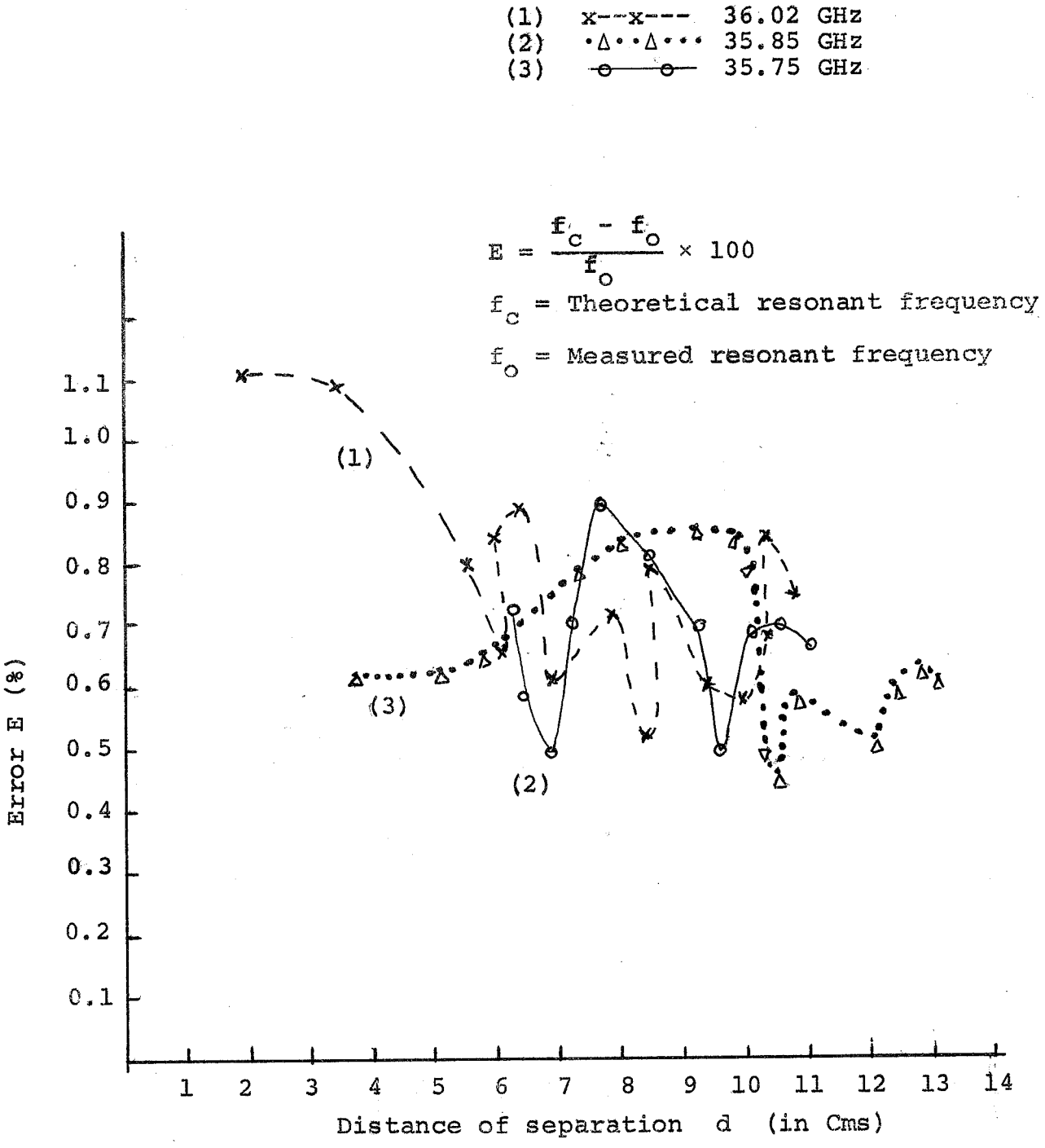

Fig. 4. Percentage error E versus distance of separation.

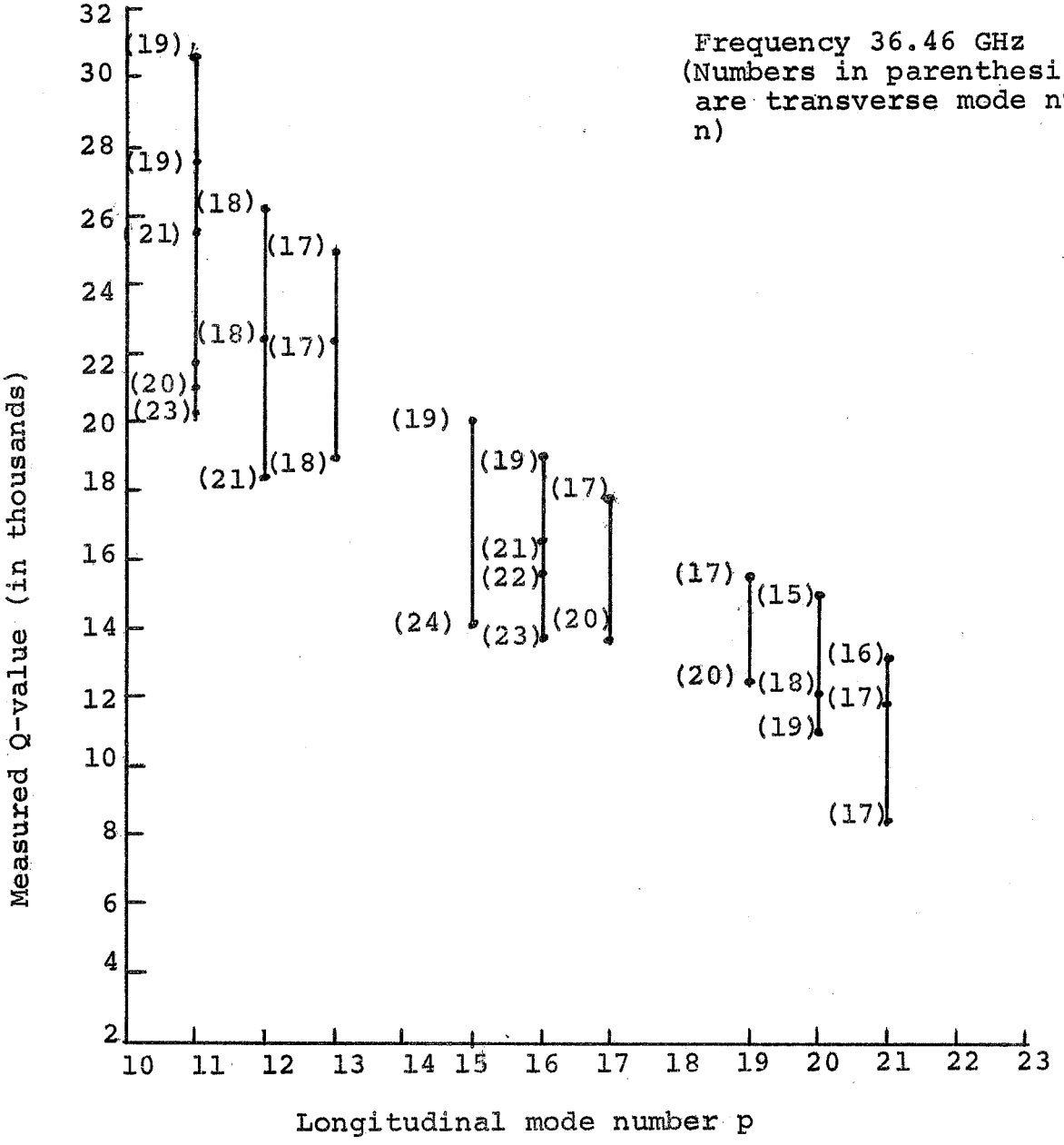

Fig. 5 Quality factor Q versus longitudinal mode number p

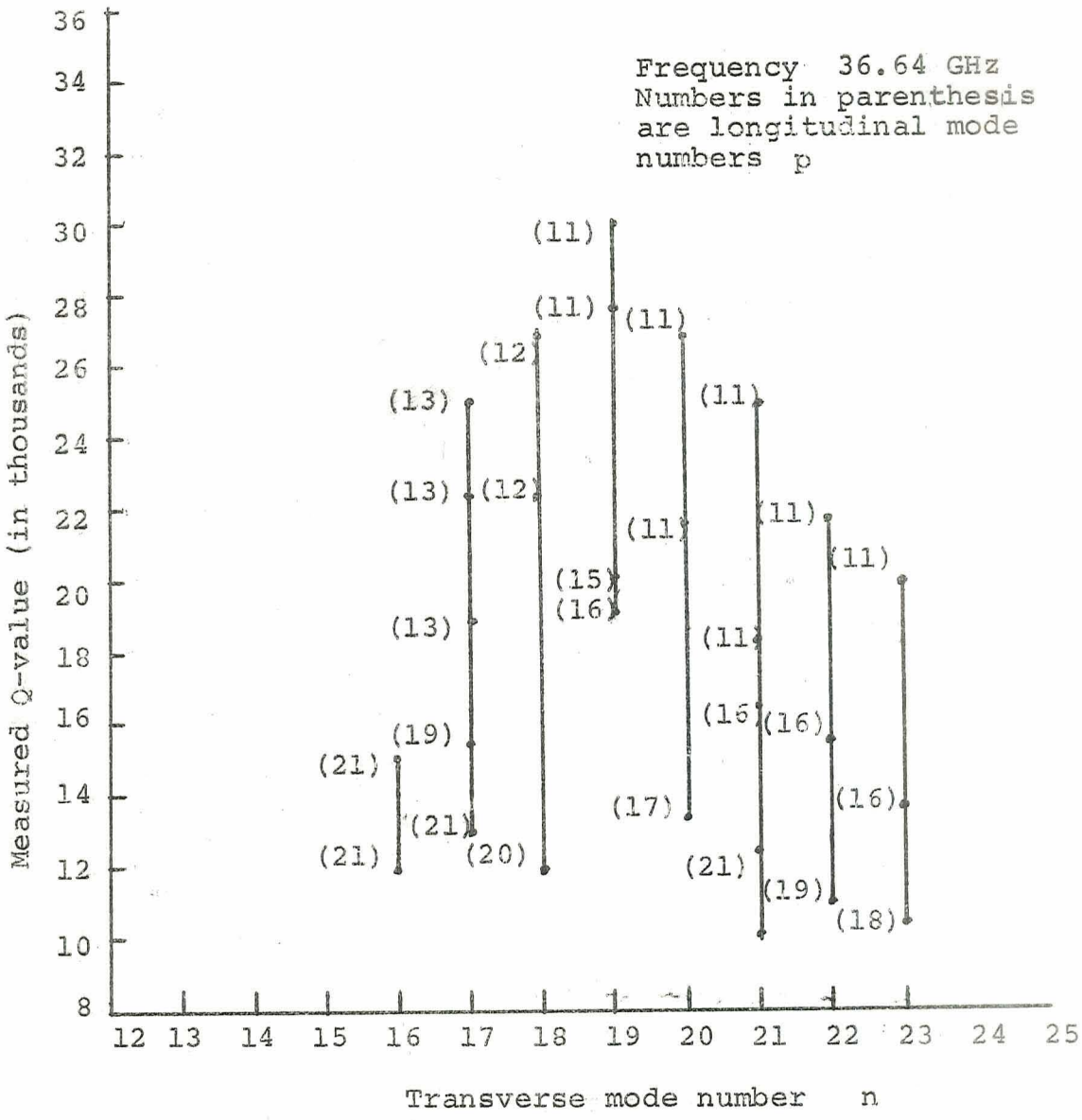

Fig. 6 Quality factor Q versus transverse mode number n.

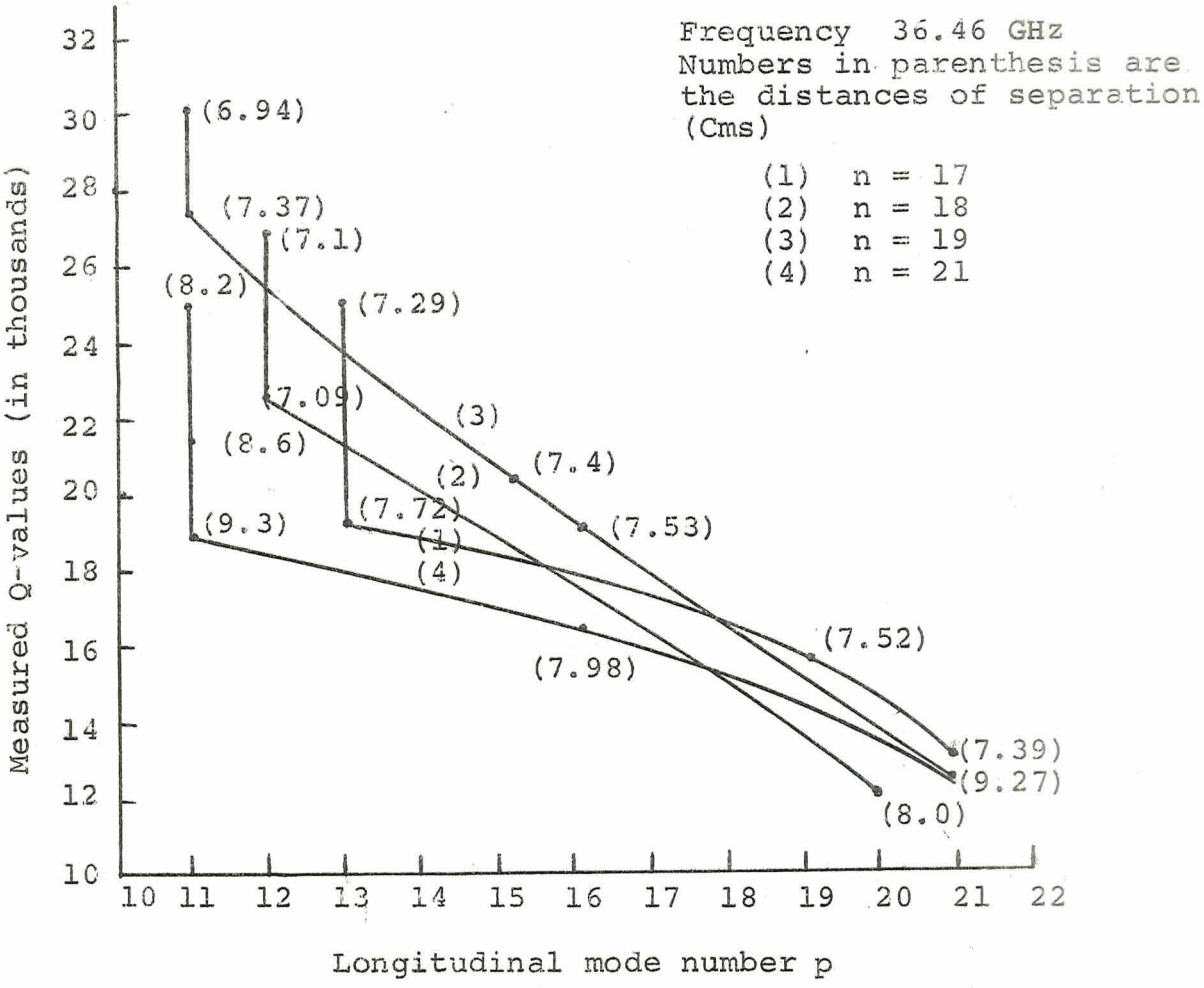

Fig. 7 Q-values in terms of longitudinal and transverse mode numbers for varying separation d.